Engineering and Technology Journal e-ISSN: 2456-3358

Volume 09 Issue 08 August-2024, Page No.- 4787-4794

DOI: 10.47191/etj/v9i08.25, I.F. – 8.227

Application of Geographic Information System (GIS) for Hypsometric Analysis of a Bicol River Basin Area

Raymundo V. Romero

Professor VI, Partido State University, Goa, Camarines Sur, Philippines

ABSTRACT: Hypsometric analysis was employed to assess the erosion status of watersheds. This is necessary to check erosion, conserve water and to implement better land management practices. This study applied the Geographic Information System (GIS) to conduct a hypsometric analysis in a vital source of surface water of Bicol River Basin particularly the Lake Buhi catchment area. Significantly, the fundamental hypsometric parameters were described. The proportions of altitude to a particular land area using the hypsometric integral (HI) was illustrated. It was concluded that application of GIS was instrumental to describe the different topographic features such as the erosional, residual and depositional features reflected in the contour and hill shade maps. It was found that the area proportion is decreasing while the elevation interval is increasing. The hypsometric curves are at old dissected, eroded landscape except for P-1 that exhibits maturely dissected landform. The HI reflected that they are at old dissected, eroded landscape. The result of this study may be considered for several applications: it will serve as an aid in the implementation of necessary measures to conserve water and soil resources for the catchment's long-term development; the approach presented may be used in assessing other river basin for the initial characterization; practical applications are foreseen in hydrology, soil erosion and sedimentation studies; it may be used for understanding the stages of geomorphic development of other river basin; it may be used in prioritizing watershed for planning engineering measures and to mitigate the impact; the GIS approach may be used to obtain hypsometric information and in enabling the hydrologic modelling community.

KEYWORDS: GIS**,** Hypsometric Analysis, river basin, hypsometric integral, hypsometric curve, catchment area, contour

I. INTRODUCTION

Watershed is a geographical dynamic unit which covers all land that contributes runoff to a common outlet [1], making it as the area that collects precipitated water to flow [2]. It is through the hypsometric study that the distribution of the ground surface area of a landmass with respect to elevation were analysed as the relative insight to the past movement of the soil that were compared through the hypsometric curve [3]. Hypsometric analysis expresses the complexity of denudational processes and the rate of morphological changes making it useful to comprehend the erosion status and prioritize for undertaking soil and water conservation measures [4]. Although, there are numbers of quantitative analysis that are used to calculate the topography of the watershed it is difficult to analyse the result without using the suitable technique [5] but it was suggested that using the hypsometric curve and the hypsometric integral are among the suited method [6]. Hypsometric analysis has been used naturally to differentiate between erosional landforms at different stages during evolutions [7]. Since hypsometric function combines the value of slope and surface area at any elevation of the basin, it might help to obtain more precise calculations derived from surface runoff in a typical basin [8]. It was once employed to assess the erosion status of watersheds considered as an essential prerequisite for integrated watershed management and prioritization. Such procedures are vital to reduce soil erosion and to implement better land management practices [9]. It has been employed recently in several investigations related to earth science such as in geology, tectonics, geomorphology, hydrology and climatology [10].

Bicol River Basin is a sub-area of the Bicol Region in eastern Philippines, consisting of two provinces-Camarines Sur and Albay with 700,000 acres of land that about half of which are arable, and nearly with 1.8 million people [11]. Among the important contributor of water in Bicol River Basin is Lake Buhi since the collected water from the catchment flows to the basin which were found vulnerable to climate change and El Niño related weather extremes making water availability highly sensitive to the patterns of changing precipitation [12].

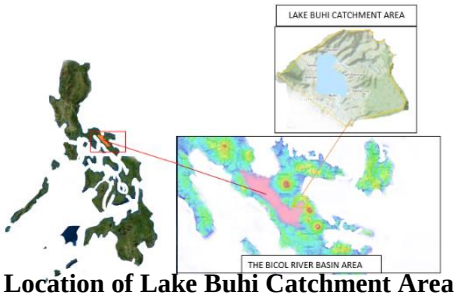

Figure 1. Location of Lake Buhi Catchment Area and Bicol River Basin in the Philippines

The lake and its watershed present classic man-in-nature governance challenges that interplay internal and external uncertainties regarding multiple uses. This results in a complex system which is difficult to manage as climate-related hazards aggravate the pressures from activities within the lake watershed [13]. The development activities in the lake and its watershed had been injurious in the past with adverse effect on the removal of forest cover, increase in number of kaingin sites, soil erosion, lake sediment, eutrophication, flooding, destruction of aquatic vegetation and species, change in lake trophic structure, etc. [14]. Assessment of erosion status is an essential prerequisite of an integrated watershed management program as it helps in selecting suitable conservation measures to check erosion and conserve water as well as in devising best management practices [15]. Hazards of debris avalanches and large landslides are significant at both active and extinct volcanoes [16].

II. OBJECTIVES

A. General Objective

The main objective of this study is to apply GIS in conducting hypsometric analysis of Lake Buhi catchment area.

B. Specific Objectives

Specifically, it aims to: describe the fundamental hypsometric parameters of the catchment area considering the following: a) contours, b) hillshade, and c) area and height proportion; conduct hypsometric analysis using the hypsometric curve; and illustrate the proportion of altitude to a particular land area using the hypsometric integral (HI).

III. METHODOLOGY

The portion of Bicol River Basin that was studied is the Lake Buhi Catchment area. The formation of the area was when Mt Iriga was cut by an active strike-slip fault [17], [18] which is related to the progressive deformation of the edifice by the underlying fault and gravity spreading into the Bicol River Basin. Using the geographic information system (GIS), the following steps were followed: 1) elevation range of the basin were put into one hundred (100) elevation class intervals., 2) the area (a_1) of the basin were measured above the bottom of each elevation class interval using the polygon in the measurement tab of the google earth pro. The bottom elevation started from 85.00 meters which is the normal water surface elevation of the lake as it appeared in the digital elevation map; 3) calculated the area proportion of the area (x) above the bottom of each interval by dividing the obtained area (a_1) by the total catchment area (A_c);

$$x = \frac{a_1}{A_c}$$

4) determined the relief (h) above a given elevation class interval by subtracting the basin mouth elevation (h_m) from the bottom class elevation (h_b);

$$h = h_b - h_m$$

5) determined the fraction of relief (y) that lies below the bottom of each interval by dividing the value obtained in Step 4 by the relief (H) of the basin for each elevation class interval; 6) the hypsometric curves were drawn by plotting the area proportion (x) versus height proportion (y).

The total catchment area and boundary of the lake was identified using the digital elevation map taken from the Google Earth Pro wherein the highest elevation indicated the boundary of the catchment were marked the boundary lines. The boundary lines are the highest portion that during rainfall, the precipitation water will flow towards the lake. With those lines, the catchment area was divided into four quadrants using the geographic coordinate system as the boundary lines with N13°27' for latitude and E123°31'12" for longitude. The four areas were marked as P-1, P-2, P-3 and P-4. The location and the boundary lines are shown in Figure 2.

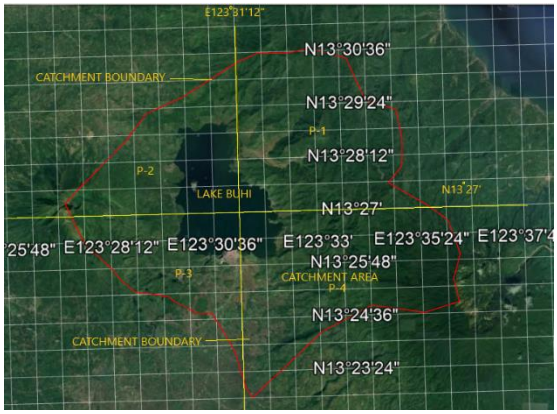

Figure 2. The catchment area and the boundary lines

Hypsometric analysis aims at developing a relationship between horizontal cross-sectional area of the watershed and its elevation in a dimensionless form wherein the digital contour map was used to generate the data required for relative area and elevation analysis [19]. The digital elevation model (DEM) and Geographical Information System (GIS) were utilized to produce contour and hill shade maps. Contour representation was used as an excellent visual abstraction of the Earth's surface due to fact that they offer enough detail at a minimal graphical load. The production techniques were in concert with the available tools and methods of data collection and graphic drawing using the latest method of producing contours from digital elevation models (DEMs) [20]. Hillshade map was considered as a convenient means in predicting woodland dieback in arid and semi-arid regions. Using the hill shade criterion increased the accuracy and scope of the analysis of changes in plant ecosystem parameters against climate change and global warming [21] likewise, it was used to produce reliable landslide maps characterized by old landslides [22]. Several parameters were used to interpret the hypsometric curves and hypsometric index in assessing the evolutionary status. The catchment area

is in the youth stage if the curve is convex upward while it is in mature stage if it is in S-shaped which is concave upward at high elevation and convex downward at low elevations. It is at old stage if it is concave upward [23]. Although the hypsometry of the catchment area was illustrated graphically through the hypsometric curves it was analysed quantitatively by computing the hypsometric integral, [24], [25] using the elevation relief ratio method [26] expressed by the following equation:

$$HI = \frac{E_{wm} - E\min}{E_{\max} - E_{\min}}$$

where HI is the hypsometric integral, E_{wm} is the weighted mean elevation of the catchment area, E_{max} is the maximum elevation and E_{min} is the minimum elevation. The following is the formula for computing E_{wm} [27]:

$$E_{wm} = \frac{\sum NiEi}{\sum Ni}$$

where Ni is the number of pixels corresponding to elevation Ei. However, Ni can also consider the area above the bottom of elevation interval corresponding to the relief Ei. The results were interpreted using the following criteria [8]: a) the area will be not in equilibrium (youthful) stage when HI ≥ 0.60, equilibrium (mature) stage when 0.35 ≤ HI< 0.60, and monadnock (old stage) when HI < 0.35.

IV. RESULTS AND DISCUSSION

By applying the steps being introduced, GIS was applied obtaining the following results:

A. Hypsometric parameters

Hypsometric parameters were described according to the following: contour and the hill shade characteristics, area and height proportions, and figure of the hypsometric curves.

Contours. Elevation contours were produced for accurate elevation assessment which is needed for perception of landforms. Contour representation is an excellent visual abstraction of the Earth's surface since they offer enough detail at a minimal graphical load while the production techniques shave changed significantly in concert with the available tools and methods of data collection and graphic drawing using digital elevation models (DEMs). This makes the creation of contours free from laborious manual work [20]. The following are the contour map of parts and the whole area as well.

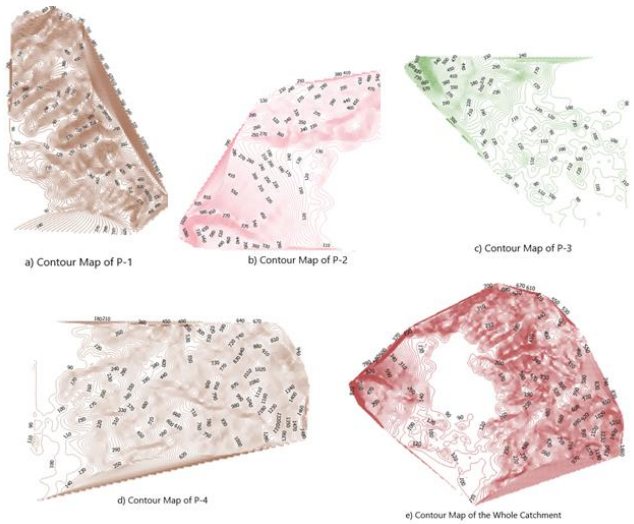

Figure 3. Contour maps of identified parts and the whole catchment area

Contoured appearances are of different kinds of topographic features [28]. They are the erosional features which are common in P-1, P-2, P-3 and P-4. These may be formed by stream courses that include valleys, gullies, washes, and gorges. Residual features are seen in P-3 showing that the area has resisted erosion effectively and have remained somewhat in their original state. Depositional features in areas that indicate deposits of soil, rock, and other material may be built up by carrying agents like streams, winds, and volcanoes.

Hillshade. Hillshade maps are shown in Figure 4. These are areas that are usually indicated with landslide [22]. Shallow landslides are easier to detect on aerial photographs while deep-seated landslides are easier to detect on Light Detection and Ranging (LIDAR). It was mentioned that it could even be detected twice as many deep-seated landslides on hillshade maps derived from LIDAR in a densely forested region [29]. Similarly, the topographic features that are seen from the contour maps are also reflecting in the hillshade maps such as the erosional, residual and the depositional features in different parts of the catchment area. Smooth surfaces that are

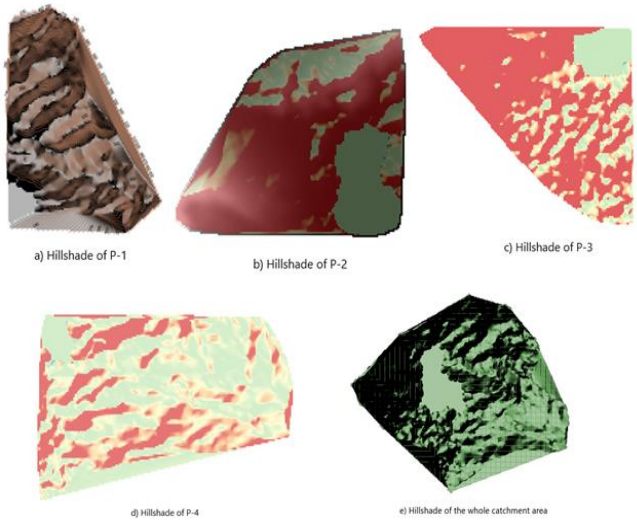

Figure 4. The hillshade maps

seen from P-2 and P-3 are representing the slope of Mt. Iriga while other features represent the debris avalanche deposits (DAD) that may be caused by the regional basement faults related to the tectonic or volcanic seismicity [30]. The DAD that dammed the Barit River and formed Lake Buhi shows no evidence of contemporaneous magmatic activity, suggesting of a non-volcanic trigger for the sector collapse event that happened in 1628 AD [31] wherein it was estimated to have an age [32] of about 500 AD. The hillshade of P-1 and P-4 is characterized by valleys, gullies, washes, and gorges as part of the slope of adjoining Mt. Malinao.

Area Proportion and height proportion. Shown in table 5 are the area and height proportion of the whole catchment area. The highest elevation is 1548.00 meters. Starting from the water level elevation of the lake and based from the 100 meters elevation interval, the area proportion is decreasing

Table 5. Tabular Computation for Area proportion and height proportion for the whole catchment

Elevation Interval (m)	Area (km^2) above bottom of interval (a_1)	Area proportion $x = \frac{a_1}{A_c}$	Lower interval elevation – mouth elevation (h)	Height proportion $y = \frac{h}{H}$
85-100	131.13	1	0	0
100-200	115.39	0.87997	15	01
200-300	77.47	0.59079	115	0.079
300-400	60.45	0.46099	215	0.147
400-500	45.30	0.34546	315	0.215
500-600	28.80	0.21963	415	0.284
600-700	19.00	0.14489	515	0.352
700-800	14.86	0.11332	615	0.42
800-900	11.33	0.0864	715	0.489
900-1000	8.66	0.06604	815	0.557
1000-1100	6.57	0.0501	915	0.625
1100-1200	4.82	0.03676	1015	0.693
1200-1300	2.92	0.02227	1115	0.762
1300-1400	1.77	0.013498	1215	0.83
1400-1500	0.49	0.00373	1315	0.899
1500-1548	0.45	0.00343	1415	0.967

while the elevation interval is increasing. From the lowest elevation interval, it decreased from 1 down to the highest elevation interval which is 0.00343. Inversely, the height proportion increased from 0 to 0.967. The two ratios involved from the presented tables are needed in plotting against each other on a graph in which the ordinate represents the ratio of relative elevation (h/H) and the abscissa represents the ratio of relative area (a/A). The relative elevation which is useful to visualize fluvial landforms but may be hard to discern from an aerial image or DEM alone was computed as the ratio of the height of a given contour (h) from the base plane to the maximum basin elevation (H) while the relative area was obtained as a ratio of the area above a particular contour (a) to the total area of the basin above the outlet (A), however, the value of relative area (a/A) is in a range from one to zero and one at the lowest point in the drainage basin (h/H = 0) and zero at the highest point in the basin (h/H = 1) [33]. Among the techniques applied in computing the relative elevation include the refinement of a given coarse digital elevation model using higher resolution multispectral imagery. In this kind of application, the given digital elevation model essentially calibrates the elevation growing process so that the resulting refinement constitutes a smart interpolation process [34].

B. Hypsometric curve

Using the area and height proportions per elevation interval of the identified parts, the hypsometric curves were produced. The figure shows that the hypsometric curve formed in P-1 is in S-shape. It indicates that it is in a maturely dissected landform. In the hypsometric curve with an S-type, the elevation frequencies concentrate in the intermediate elevations which is observed in pure alluvial plains [35].

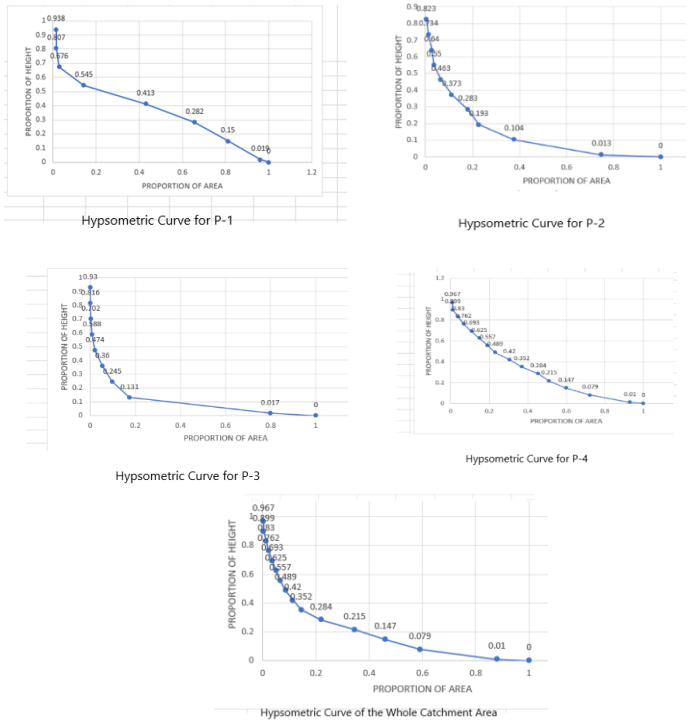

Figure 5. Hypsometric Curves representing the different portions and the whole catchment area

When the ranges reach the culminating stage, the hypsometric curve will be S-type, and the elevation frequencies will be in the intermediate altitudinal classes with a normal distribution. It was cited [36] that the hypsometric curve of a mountain changes from a concave curve to an s-shaped curve in accordance with the increase in mountain altitude while the succession of the hypsometric curve during concurrent tectonics and denudation is the reverse of Strahler's diagram. However, it was observed [37] that the combination of convex-concavo and S-shape of the hypsometric curves are

due to the soil erosion from the sub-watersheds resulting from the incision of channel beds, down slope movement of topsoil and bedrock materials, washout of the soil mass and cutting of streams banks.

The hypsometric curves that are formed are in concave shape which indicate that majority of the basin area lies at comparatively low relief and is associated with old dissected, eroded landscape. This demonstrates that the landscape was shaped either by the climate, tectonic uplift or the channel networks draining them [38], [39] during the early years. The area has a volcano known as Mt. Iriga which is well known for its southeast elongated avalanche scar generated by a 1.5 km^3 collapse that spread as a rockslide debris avalanche over an area of 70 km^2 [40]. The debris avalanche deposits dammed a river and formed Lake Buhi. Judging from the surrounding areas unaffected by the debris avalanche, and from sketchy historical reports, the Buhi area before the avalanche was relatively flat valley as it was written that the lake did not come into existence until half the mountain fell in [41]. The data can be used to infer the stage of development of the drainage network and can be used as a tool to differentiate between tectonically active and inactive areas [42], [43].

C. Hypsometric Integral

The computed Hypsometric Integral and interpretated geological stages are shown in Table 6.

Table 6. Hypsometric Integral and geological stages

Portion	Area (Km^2)	Min. elevation (m)	Max. elevation (m)	Weighted Mean elevation (m)	HI	Stage
P-1	40.40	85	847.00	241.32	0.205	Old
P-2	24.73	85	1196.00	252.05	0.150	Old
P-3	22.57	85	961.00	159.64	0.085	Old
P-4	43.43	85	1548.00	441.84	0.244	Old
WC	131.13	85	1548.00	339.23	0.174	Old

The geological stages are mostly at old ages based from the estimation of HI. However, there is discrepancy in the result for P-1 compared to the hypsometric curve which was interpreted at matured stage. The discrepancies could be attributed to some conflicts in measurement using the polygon system for the presence of soil erosion in the catchment area could make difficult to measure the cutting of channel beds, downslope movement of topsoil and bedrock material, washed-out soil mass and cutting of stream banks [44]. Using Google Earth Pro is very good time saving tool for measuring the area of closed boundary compared to field measurements but the accuracy of the measurements decreases as station point's increases. The qualitative shape of the hypsometry curve and the hypsometric integral are generally independent of DEM spatial resolution based on data with varying spatial resolution ranging [45]. The HI difference between the watershed boundary and the watershed reflects the relative amount of material that has been eroded within the basin, while the HI difference between the watershed and the main gully reflects the amount of material that can still be eroded. A single watershed HI can only simply determine the period of erosion development so that by referring to these two indicators, the development of the watershed can be further quantified in concrete terms [46].

CONCLUSIONS

This study concluded that the application of GIS was instrumental to describe the different topographic features like the erosional, residual and depositional features reflected in the contour and hillshade maps. It was found that the area proportion is decreasing while the elevation interval is increasing in the area being studied. The hypsometric curves for all parts are at old dissected, eroded landscape except for P-1 that exhibits maturely dissected landform while the HI reflected that they are at old dissected, eroded landscape. The result of this study could be considered for several applications: it can serve as an aid in the implementation of necessary measures to conserve water and soil resources for the catchment's long-term development [47], [48], [49]; the approach presented may be used in assessing other river basin for initial characterization of landforms [50]; erosion control measures and land utilization planning can be done more effectively from topographic analysis where hypsometric qualities are quantitively stated [51], [27]; practical applications are foreseen in hydrology, soil erosion and sedimentation studies [8]; the approach may be used for understanding the stages of geomorphic development of other river basin [52]; the use of hypsometric integral could be highlighted for prioritizing watershed for planning engineering measures and to mitigate the impact [53]; the automated GIS approach may be used to obtain hypsometric information and calculate the associated statistical attributes [54].

ACKNOWLEDGMENT

The researcher would like to acknowledge the support extended by the PSU administration through the leadership of President Dr. Arnel B. Zarcedo, Vice President for Research and Extension Patricia Candelaria and Research Director Luisa Lanciso when it comes to financial and moral obligation.

REFERENCES

1. Sharma SK, Mishra N & Gupta A., (2007), Morphometric analysis of Ultala Naia watershed using GIS technique, Sci-fronts, (1), 178-0185
2. Sharma, SK, Gajbhiya, S, & Tignath, S., (2015), Application of principal component analysis in grouping geomorphic parameters of a watershed for hydrological modelling. Applied Water Science, 5(1), 89-96

3. Raman Mehar , M. K. Verma, R. K. Tripathi, O, (2018), Hypsometric analysis of Sheonath River Basin, Chhatisgarh, India : A remote sensing and GIS Approach, International Journal of Engineering Research & Technology, 7(10)
4. ShaIlesh Kumar Sharma, Sarita Gajbhiye Meshram,Rupesh Jairam Patil and Sanjay Tignath, (2016), Hypsometric analysis using Geographical Information System of Gour River Watershed,
5. Jabalpur, Madhya Pradesh, India, Current World Environment, 1(1), 56-64
6. Ramu, Mahalingam B., (2012), Hypsometric properties of drainage basin in Kamatka using geographical information system, New York Science Journal, 5(12)156-158
7. Weissel, JK, Pratson LF,. Malinverno, A., (1994), The length-scaling properties of topography, Journal of Geophysical Research, 99, 13997-14012
8. Strahler, (1952), Hypsometric (area-altitude) analysis of erosional topography, Geological Science of Amer Bulletin, 63, 1117-1142
9. Singh, O. (2009) Hypsometry and Erosion Proneness: A Case Study in the Lesser Himalayan Watersheds. Journal of Soil and Water Conservation, 8, 53-59.
10. Masek, JG, Isacks, BL, Gubbels, TL & Fielding EJ, (1994), Erosion and tectonics at the margins of continental plateau, Journal of Geophysical Research, 99, 13941-13956
11. Dennis A. Rondinelli, (1980) Spatial Analysis for Regional Development: A Case Study in the Bicol River Basin of the Philippines, In I.D.R. Furtado, Terry B. Grandstaff & Kenneth Ruddle, (Eds), The United Nations University Resources Systems Theory and Methodology Series, United Nations University Press
12. Rasu Eeswaran, Amor V.M. Ines, Eunjin Han, Bradfield Lyon, Kye Baroang and Agnes Rola, (2017, October 23-25), Modeling water management options for Lake Buhi in Bicol River Basin of the Philippines under climate change scenarios, ASA-CSSA-SSSA Annual Meeting, Tampa, Florida.
13. Dulce D. Elazegui, Agnes C. Rola & Erica Allis (2016), Enhancing institutional dynamics for multiple uses of water amidst climate-related risks: The case of Lake Buhi, Philippines. Lakes and Reservoirs, 21(3), 224-234
14. Doracle B. Zoleta, (1987), From the mountains to the lakebeds: resource problems and prospects in Buhi watershed, Camarines Sur, Philippines, Yearbook of the Association of Pacific Geographers, 49, 139-153
15. Shailesh Kumar Sharma, Sarita Gajbhiye & Sanjay Tignath, (2018), Hypsometry analyssis for assessing erosion status of watershed using Geographical Information System, Hydrologic Modeling, 263-276
16. Engielle Mae Paguican. (2012). The structure, morphology, and surface texture of debris avalanche deposits: field and remote sensing mapping and analogue modelling. Earth Sciences. Université Blaise Pascal-Clermont-Ferrand II.
17. Aurelio, M. A., Barrier, E., Gaulon, R., and Rangin, C. (1997). Deformation and stress states along the central segment of the Philippine Fault: implications to wrench fault tectonics. Journal of Asian Earth Sciences, 15(2-3), 107–119.
18. Lagmay, A. M. F., van Wyk de Vries, B., Kerle, N., and Pyle, D. M. (2000). Volcano instability induced by strike-slip faulting. Bulletin of Volcanology, 62(4-5):331–334
19. SFR Khadri & Chaltanya Pande, (2014), Hypsometric analysis of the Mahesh River Basin in Akola and Buldhana Districts using remote sensing and GIS technology, International Multidisciplinary Research Journal, 3(8),
20. Pyry Kettunen, Christian Kosky, & Juha Oksanen, (2017), A design of contour generation for topographic maps with adaptive DEM smoothing, 3(1), 19-30
21. Ali Najafifar, Jaafar Hosseinzadeh & Abdolali Karamshahi, (2019), The role of hillshade, aspect and toposhape in the woodland dieback of arid and semi-arid ecosystems: a case study is Zagros woodlands of Ilam Province, Iran, Journal of Landscape Ecology, 12(2), 79-91
22. M. Van Den Ecckhaul, J. Poesen, G. Verstraeten, V. Vanacker, J. Mocyersons, J. Nyssen, L.P.H. Van Beek, (2005), The effectiveness of hillshade maps and expert knowledge in mapping old deep-seated landslides, Geomorphology, 67, 351-363
23. Sunil Kumar, Chauniyal, D.D. & Surajit Dutta, (2016), Morphometric analysis of Rupin Drainage Basin in Western Himalaya: using geo-spatial techniques, International Journal of Current Research, 8(16), 40110-40117
24. Hurtrez, J.E., Sol, C. and Lucazeau, F. (1999) Effect of Drainage Area on Hypsometry from Analysis of Small Scale Drainage Basins in the Siwalik Hills (Central Nepal). Earth Surface Processes and Landforms, 24, 799-808
25. Bishop, M., Shroder, J., Bonk, R. and Olsenholler, J. (2002) Geomorphic Change in High Mountains: A Western Himalayan Perspective. Global Planetary Change, 32, 311-329
26. Pike, R.J. & Wilson S.E., (1971), Elevation-relief ration hypsometric integral and geomorphic area-altitude analysis, Geological Society of America Bulletin, 82, 1079-1084

27. Mounesh, Chanabasanagouda S. Patil, (2019) Hypsometric Analysis of Ghataprabha Sub Basin of Krishna River Basin, Karnataka, India, International Journal in Applied Science and Engineering Technology, 7(5), 2288-2293
28. John B. Rowland, (1955), Features shown on topographic Maps, Geological Survey Circular 368, Washington DC.
29. Haugerud, R.A., Harding, D.J., Johnson, S.Y., Harless, J.L., Weaver, C.S., Sherrod, B.L., 2003. High resolution Lidar topography of the Puget Lowland, Washington: a bonanza for earth science. GSA Today 13 (6), 9.
30. E.M. R. Paguican, B. van Wyk de Vries & A.M. F. Lagmay, (2012), Volcan-tectonic controls and emplacement kinematics of the Iriga debris avalanches (Philippines), Bulletin of Volcanology, 74, 2067-2081
31. Aguila LG, Newhall CG, Miller CD, Listanco EL (1986) Reconnaissance geology of a large debris avalanche from Iriga volcano Philippines. Philippine J Volcano 3, 54–72
32. Belousov A, Belousov M, Listanco E (2011) The youngest eruptions and edifice collapse of Iriga volcano, Philippines. IUGG General Assembly, Melbourne
33. Fuzal Ahmed & Srinivasa Rao, (2016), Hypsometric analysis of the Tuirini drainage basin: A geographic informatijon system approach, International Journal of Geomatics and Geosciences, 6(3), 1685-1695
34. S. Wang, R.M. Haralick & J. Campbell, (1984), Relative elevation determination from LandSat imagery, Photogrammetria, 39(1984), 193-215
35. Yen-Chieh Chen, Heng Tsai, Quo-Cheng Sung & Tsung-Yen Wang, (2020), Hypsometric curve patterns and elevation frequency histograms of active orogen, Journal of Geology and Geoscience, 4(1)
36. Ohmori H (1993) Changes in the hypsometric curve through mountain building resulting from concurrent tectonics and denudation. Geomorphology 8, 263- 277
37. Shailesh Kumar Sharma, Sanjay Tignath, Sarita Gajbhiye & Rupesh Patil, (2013), Use of geographical system in hypsometric analysis of Kanhiya Nala Watershed, International Journal of Remote Sensing & Geoscience, 2(3), 30-35
38. Hooshyar, M., Singh, A., Wang, D., & Foufoula-Georgiou, E. (2019). Climatic controls on landscape dissection and network structure in the absence of vegetation. Geophysical Research Letters, 46. https://doi.org/10.1029/ 2019GL082043
39. Willgoose, G. (1994). A statistic for testing the elevation characteristics of landscape simulation models. .Journal of Geophysical Research, 99(B7), 13,987–13,996.
40. Loreto G. Aguila, Christopher G. Newhall, C. Dan Miller & Eddie L. Listanco, (1986), Reconnaissance geology of a large debris avalanche from Iriga volcano, Philippines. Philippine J Volcano. 3, 54-72
41. Jagor, F., (1873) Reisen en den Philippinen: Berlin, Wiedmannsche, Buchhandlung, 381p.
42. Keller E A and Pinter N 1996 "Active tectonics: Earthquakes Uplift and Landscapes"; Prentice Hall, New Jersey.
43. G. Sarp, V. Toprac, & S. Dusgun, (2011), Hypsometric properties of the hydraulic basins located on western part of Nafs, 34th International Symposium on Remote Sensing of Environment, Sydney, Australia
44. Anurag Malik & Anil Kumar, Use of GIS for hypsometric (area-elevation) analysis of Gagas watershed (Uttarakhand), (2019), 46(3), 481-485
45. Hurtrez, J. E., C. Sol, and F. Lucazeau, Effect of drainage area on hypsometry from an analysis of small-scale drainage basins in the Siwalik Hills (central Nepal), Earth Surf. Processes Landforms, 24(9), 799– 808, 1999.
46. Duan Y, Pei X and Zhang X (2022) The Hypsometric integral based on digital elevation model for the area west of Lvliang Mountains in Loess Plateau, Shanxi, China. *Front. Earth Sci.* 10:827836. doi: 10.3389/feart.2022.827836
47. Padala Raja Shekar & Aneesh Mathew, (2022), Evaluation of morphometric and hypsometric analysis of Bagh River Basin using remote sensing and geographic information system techniques, Energy Nexus, 7(2022), 1-12
48. Ahmed, Fuzal. (2016). Hypsometric analysis of the Tuirini drainage basin: A Geographic Information System approach. International Journal of Geomatics and Geosciences. 6. 1685-1695.
49. Kusum Pathak, Medha Jha, Sanjay Tignath, S.K Sharma (2019), Hypsometric Analysis of the Berne River Watershed using Geographical Information System, International Journal of Scientific Development and Research, 4(9), 83-87
50. Torrefranca, Imelida & Otadoy, Roland Emerito & Tongco, Alejandro. (2021). χ-maps and Hypsometric Analysis for River Basin Management and Prioritization: The Case of Bohol River Basins, Central Philippines. 10.21203/rs.3.rs-196247/v1.
51. Raman Mehar, M.K. Verma, R.K. Tripathi, (2018), Hypsometric Analysis of Sheonath River Basin, Chhatisgarh, India: A remote sensing and GIS approach, International Journal of Engineering Research and Technology, 7(10), 116-121
52. Babu, K.J., Sreekumar, S.S., Aslam, A., & Midhun, K.P. (2014). Hypsometry and Geomorphic

Development of a Watershed: A Case Study from South India. International Journal of Science and Research, 3(10), 1495-5000

53. Kusre, B.C. Hypsometric analysis and watershed management of Diyung watershed in north eastern India. *J Geol Soc India* 82, 262–270 (2013). https://doi.org/10.1007/s12594-013-0148-x
54. Luo, Wei. (1998). Hypsometric analysis with a Geographic Information System. Computers & Geosciences - COMPUT GEOSCI. 24. 815-821. 10.1016/S0098-3004(98)00076-4.